Corrosion behaviors of nanocrystalline and conventional polycrystalline copper

J. K. YU, E. H. HAN*, L. LU, X. J. WEI
State Key Laboratory for Corrosion and Protection of Metals, Institute of Metals Research, the Chinese Academy of Sciences, Shenyang 110016, People's Republic of China
E-mail: ehhan@imr.ac.cn

M. LEUNG
Department of Mechanical Engineering, The University of Hong Kong, Pokfulam Road, Hong Kong

Nanocrystalline materials have been of high technological and scientific interests because of their unique physical, chemical and mechanical properties that can be useful for extensive applications. Corrosion properties are also affected by nanocrystallization. This is generally attributed to the unique internal microstructure of nanocrystalline materials with many grain boundaries, which may amount to as much as 50% by volume. It has also been shown that the degree of corrosion is related to the microstructure in terms of crystallographic texture, porosity, impurities and triple junctions [1]. For passive alloys, local break down of passive layer may lead to pitting corrosion. The performance of passive film formed on a nanocrystalline material could be very different from that on a conventional crystalline material [2]. Improved corrosion resistances have been reported for nanocrystalline $Al_{90}Fe_5Gd_5$ and $Al_{87}Ni_{8.7}Y_{4.3}$ alloys [3], nanocrystalline brass [4], nanocrystalline $Fe_{32}Ni_{36}Cr_{14}P_{12}B_6$ and $Fe_{72}Si_{10}B_{15}C_{13}$ super films [5], nano 304 stainless steel [6] and nanocrystalline Ni-5Cr-5Al coating [7]. On the other hand, studies have shown reduced corrosion resistances for nanostructured $Cu_{90}Ni_{10}$ alloy [8] and nanostructured 99% Ni [9], attributed to reduced passivation kinetics and instability of passive films.

In the present work, the nanocrystalline copper sample was fabricated by means of electrodeposition technique with an electrolyte of $CuSO_4$. Nanocrystalline copper was deposited on a Ti substrate to a thickness of about 2 mm. The purity of the Cu cathode was about 99.99 wt%. The current density in the present electrodeposition process was about 13 mA/cm^2 with a double pulsed power. The acidity of the electrolyte was about 0.9 mol/L. The bath temperature was kept at 20 °C. The electrolyte was agitated every 20 min [10]. Potentiodynamic polarization curves were plotted at a scan rate of 0.2 mV/s using a 3.5 wt% NaCl solution at 25 °C. A three-electrode cell system was employed. The working electrode (WE) was the copper sample and a saturated calomel electrode (SCE) was used as the reference electrode (RE). The potentials were measured via a Luggin-Haber capillary. All potentials presented in this paper were measured with respect to the SCE. The counter electrode was a 15 mm × 15 mm platinum plate. The working electrodes were immersed in 3.5 wt% NaCl solution. The solution was prepared from pure chemicals

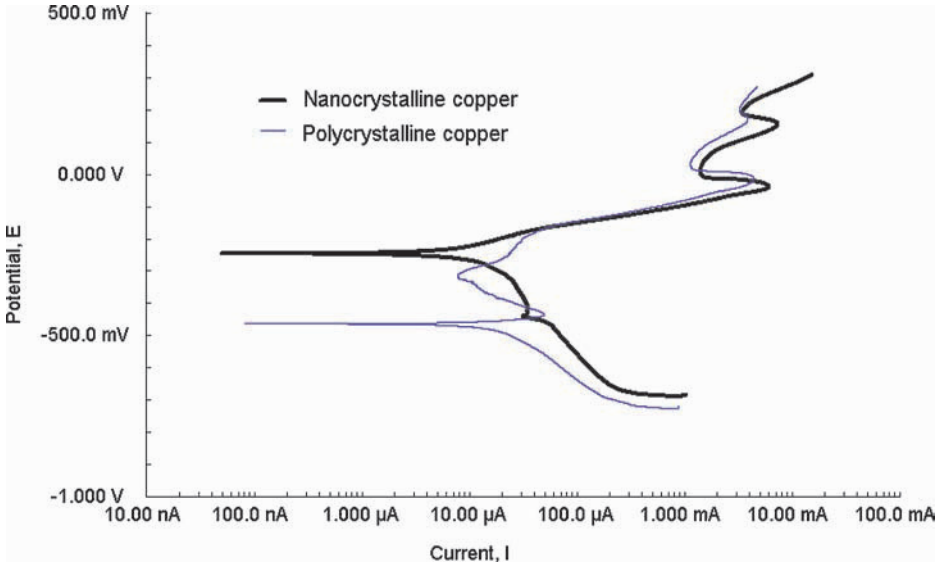

Figure 1

*Author to whom all correspondence should be addressed.

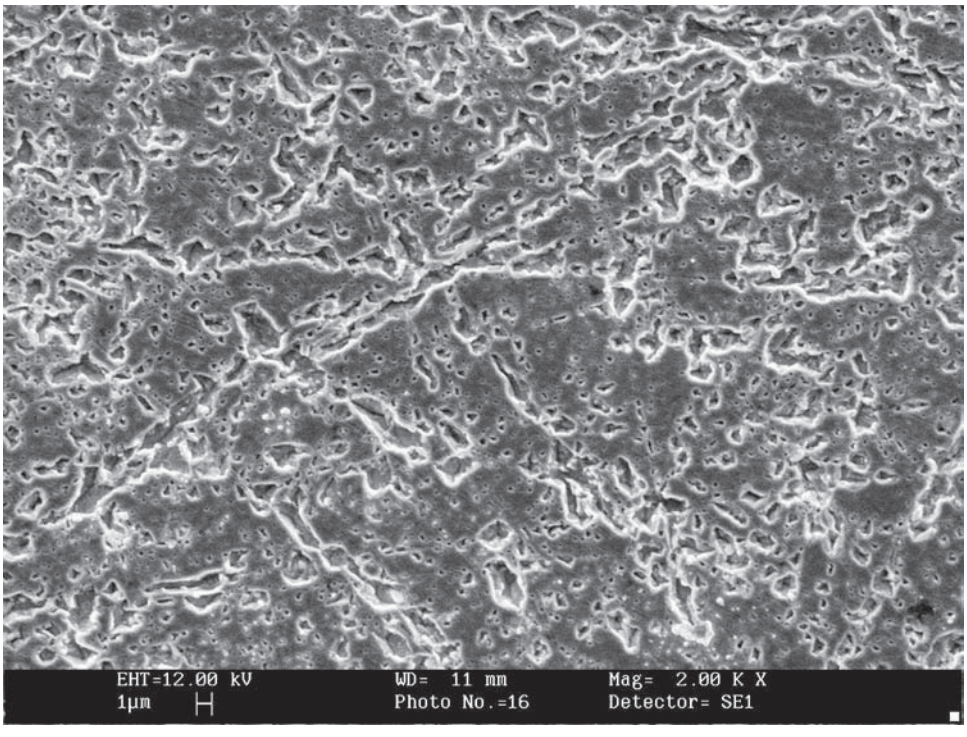

Figure 2

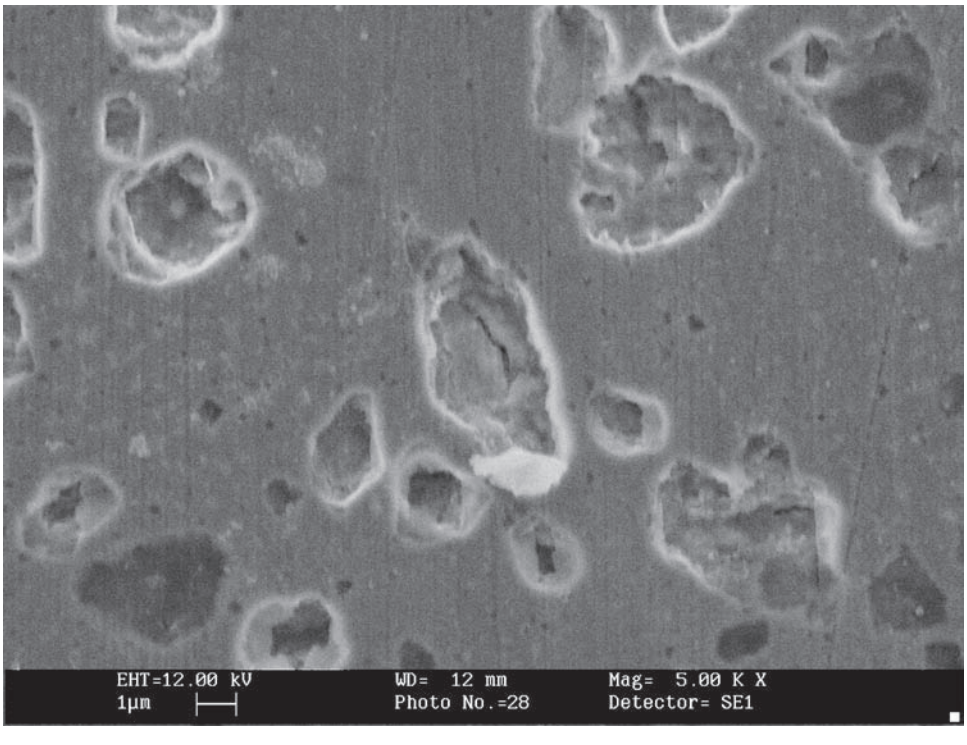

Figure 3

and deionized water. The samples were exposed to the test conditions for 2 hr to reach a steady-state open circuit potential. For the electrochemical noise measurements, a pair of copper electrodes were immersed in the test solution as the working electrodes (WE) and the noise power spectrum values were recorded against the immersion time up to 10 hr. A Gamry PC4/750 system was used to conduct the polarization and electrochemical noise measurements. Subsequently, the surface morphology of each sample was evaluated by means of Cambridge S440 scanning electron microscope (SEM).

Fig. 1 presents the potentiodynamic polarization behaviors of the nanocrystalline and polycrystalline copper electrodes. The scanning potential (E) was from −0.8 to 0.4 V at a scan rate of 0.2 mV/s. It was demonstrated that the nanocrystalline had higher corrosion potential (E_{corr}), higher cathodic current and lower anodic current. According to the Pourbaix diagram, this might be due to the formation of passive film or oxide film at the open potential in the nanocrystalline electrode system. When the potential was increased to −162.3 mV, the polarization curves of the nanocrystalline

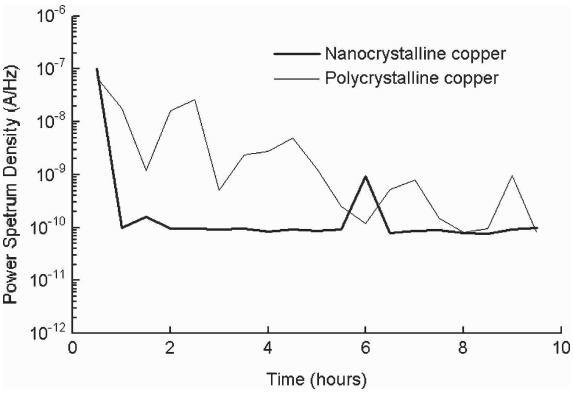

Figure 4

andpolycrystalline copper electrodes were almost overlapping each other. These results showed the overall dissolution rate at a high potential overwhelmed the structure-controlled dissolution rate at a low potential.

The surface of nanocrystalline copper has many grain boundaries, triple junctions and other defects that likely provide preferential attack sites upon exposure to a corrosive environment at a cathodic potential. However, as shown in the SEM micrographs in Figs 2 and 3, the nanocrystalline copper electrode exhibited less pitting corrosion attack than the polycrystalline copper electrode, after polarization from −0.8 to 0.4 V at 0.2 mV/s in 3.5 wt% NaCl solution. It is because nanocrystalline copper is apt to peptize quickly to induce colloid coagulation of copper ions to larger aggregates [11]. This characteristic might lead to a formation of a passive film, consisting of CuCl and Cu_2O [12]. The film prohibited any further corrosion on the nanocrystalline specimen. As a result, the corrosion current density at the nanocrystalline electrode surface was lower between the open circuit potential and −162.3 mV as shown in Fig. 1. When the potential became more positive, more copper dissolution was driven by extrinsic

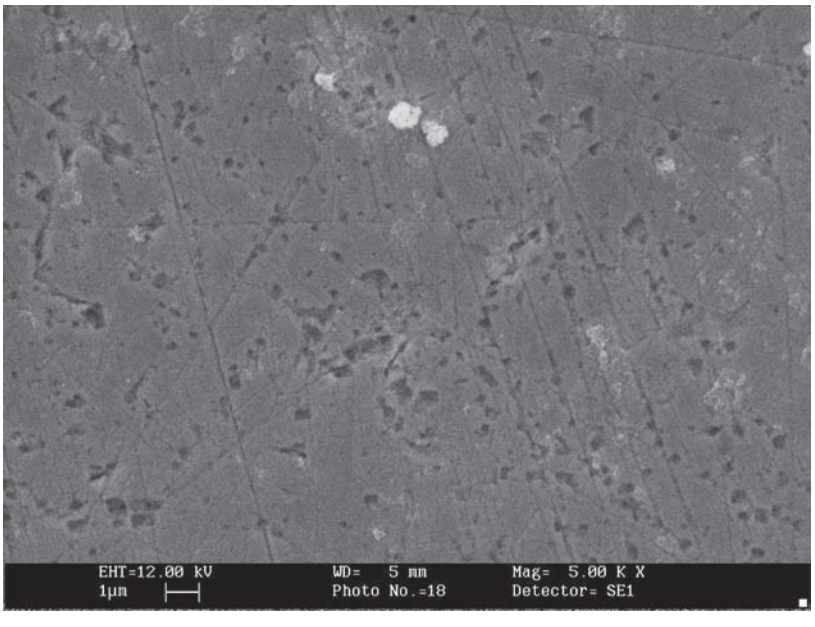

Figure 5

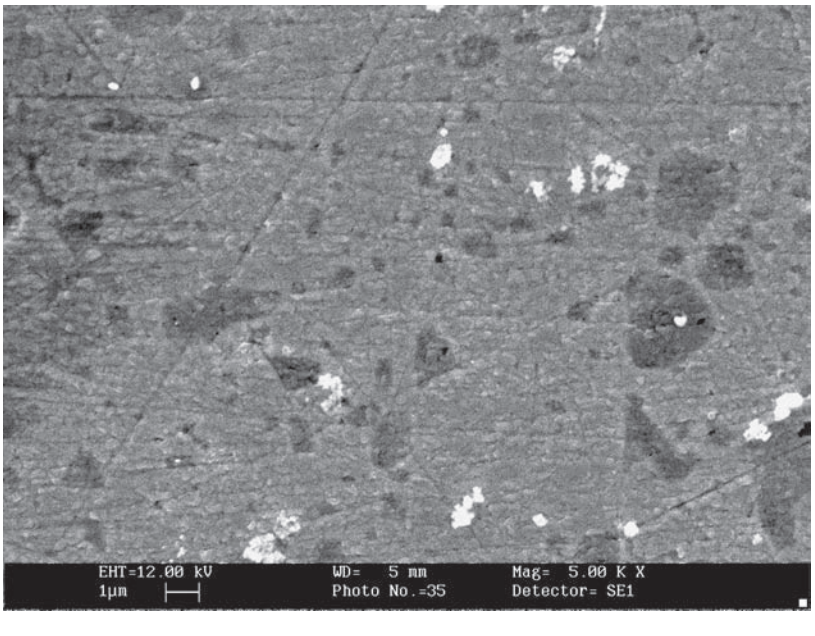

Figure 6

potential. Similar morphology of the nanocrystalline copper and polycrystalline copper can be observed in the SEM images. The pitting corrosion failure on the surface of polycrystalline copper was severer because of less active intercrystalline area. Therefore, some concentrated active anode spots yielded serious pitting corrosion.

The electrochemical noise measurements show the voltage and current fluctuations at different immersion times. In this study, the current/potential noise power spectrum density (PSD) has been analyzed. Fig. 4 shows the variation of PSD with immersion time. The sudden drop in the current noise power spectrum density on the nanocrystalline copper surface mainly resulted from the passivation process during the initial immersion. The disturbance in the current noise power spectrum density after about 5.5 hr of immersion was possibly due to the formation and repassivation of the pitted area. The fluctuating current transients and current noise power spectrum on the polycrystalline copper surface indicated the frequent initiation, growth and repassivation processes of metastable pits. It implied that stable passive film was difficult to form on the polycrystalline copper surface. The overall current noise power spectrum density of polycrystalline copper decreased gradually with the immersion time. This phenomenon can be explained by the occurrence of macroscopic pitting corrosion from the polycrystalline copper substrate. The high dissolution rate of copper prohibits the current and potential noise fluctuation when the pits are formed and recovered. The SEM images shown in Figs 5 and 6 present the localized attack on polycrystalline sample and uniform attack on nanocrystalline structured specimen, respectively.

The results of this study show that the surface of nanocrystalline copper is more active during initial immersion, that leads to the formation of a passive film quickly. The uniform passive film then protects the nanocrystalline copper from the further serious corrosion. Stable passivation does not occur on the surface of conventional polycrystalline copper. Therefore, corrosion pits, likely formed on grain boundaries, impurities, triple junctions and surface defects, are severer on a polycrystalline surface.

Acknowledgments

The work in this paper is supported by the National Excellent Doctors Fund of China and a grant from the Research Grants Council of the Hong Kong Special Administrative Region, China (Project No. HKU 1008/01E).

References

1. G. PALUMBO, S. J. THORPE and K. T. AUST, *Scripta Metall.* **24** (1990) 1347.
2. X. Y. WANG and D. Y. LI, *Electrochimica Acta* **47** (2002) 3939.
3. J. E. SWEITZER, G. J. SHIFLET and J. R. SCULLY, *Electrochimica Acta* **48** (2003) 1223.
4. L. C. WANG and D. Y. LI, *Surf. Coatings Technol.* **167** (2003) 188.
5. S. J. THORPE, B. RAMASWAMI and K. T. AUST , *J. Electrochem. Soc.* **135** (1988) 2162.
6. R. B. INTURI and Z. SZKLARSKA-SMIALOWSKA, *Corrosion* **48** (1992) 398.
7. G. CHEN and H. LOU, *Nanostruct. Mater.* **11** (1999) 637.
8. A. BARBUCCI, G. FARNE, P. MATTEAZZI, R. RICCIERI and G. CERISOLA, *Corr. Sci.* **41** (1999) 463.
9. R. ROFAGHA, R. LANGER, A. M. EL-SHERIL, U. ERB, G. PALUMBO and K. T. AUST , *Scripta Metall.* **25** (1991) 2867.
10. L. LU, N. R. TAO, L. B. WANG, B. Z. DING and K. LU, *J. Appl. Phys.* **89** (2001) 6408.
11. P. MULVANEY, in Nanoscale materials in Chemistry, edited by K. J. Klabunde (Wiley, 2001) pp. 121.
12. F. J. CORNWELL, *Brit. Corr. J.* **8** (1973) 202.

Received 6 May
and accepted 20 July 2004